Hydrogen Adsorption in Carbon Materials

M.S. Dresselhaus, K.A. Williams, and P.C. Eklund

Introduction

Recent reports of very high, reversible adsorption of molecular hydrogen in pure nanotubes,[1-3] alkali-doped graphite, and pure and alkali-doped graphite nanofibers (GNFs)[4,5] have aroused tremendous interest in the research community, stimulating much experimental work and many theoretical calculations worldwide. The U.S. Department of Energy (DOE) Hydrogen Plan has set a standard for this discussion by providing a commercially significant benchmark for the amount of reversible hydrogen adsorption. This benchmark requires a system-weight efficiency (the ratio of stored H_2 weight to system weight) of 6.5-wt% hydrogen and a volumetric density of 63 kg H_2/m^3.[6] If the encouraging experimental reports (summarized in Table I) are reproducible, it may be possible to reach the goals of the DOE Hydrogen Plan. On the other hand, the community still awaits confirmation of these experimental results by workers in other laboratories. Of additional concern is the fact that theoretical calculations[7-11] have been unable to identify adsorption mechanisms compatible with the requirements of the DOE Hydrogen Plan.

An economical, safe, hydrogen-storage medium is a critically needed component of a hydrogen-fueled transportation system. Hydrogen storage in a *carbon-based material* offers further advantages associated with its low mass density. Furthermore, fuel cell technology involving the conversion of hydrogen into protons, or hydrogen and oxygen into electric current, is being vigorously researched for both transportation and small power-plant applications.[12]

In this brief review, we first summarize several recent reports of high, reversible hydrogen adsorption in graphite, carbon nanotubes, and GNFs. This is followed by highly simplistic arguments that set a framework for discussing the conditions that might be needed to achieve the requirements of the DOE Hydrogen Plan. We then refine this basic framework by discussing a few of the recent detailed calculations and conclude with an outline of the challenges ahead.

Experimental Results

A remarkable experimental result for hydrogen storage in an absorbent carbon material was reported by Rodriguez and co-workers.[4] Molar fractions $[n(H_2)/n(C)]$ of H_2 stored at room temperature in GNFs in the range of ~1–11 were reported. The H_2 storage was accomplished at pressures well above ambient pressure (11.35 MPa) for three distinct structural types of GNFs: "tubular" (90°), "herringbone" (~45°), and "platelet" (0°), where the angle in parentheses indicates the direction of the nanofiber axis relative to the vector normal to the graphene sheets (see Table I). A graphene sheet is a layer of graphite one atom thick. The structural forms of the GNFs were obtained by varying the sample preparation conditions, but few details on these conditions were given in their report,[4] making it difficult for other researchers to duplicate their results and to confirm their validity. The GNFs exhibited lengths of 10–100 μm and cross-sectional areas from tens to hundreds of square angstroms. Although this structural information should be available from transmission electron microscopy (TEM), selected-area diffraction patterns, and image analysis, these data and images were not presented in their paper.[4] It was proposed that the hydrogen was adsorbed in "slit pores" (Figure 1) of width d_p = 3.37 Å, which is effectively the interplanar spacing between graphene sheets in the GNFs. It was found that the platelet and herringbone forms of GNFs adsorbed 4–6 times more H_2 than the tubular form. The authors proposed that the interplanar spacing d increases to accommodate one to several layers of H_2 molecules between successive graphene layers.[4] Unfortunately, no *in situ* structural data, such as the c-axis expansion, on this remarkable H_2 storage system are yet available. This report suggests adequate reversibility; for example, adsorption and desorption data on one herringbone sample exhibited ~75% reversibility at room temperature and ~0.1 MPa. The desorption was observed to be quite rapid, taking 5–10 min.

Dillon et al.[1] investigated the hydrogen-adsorption capacity of bundles of single-walled carbon nanotubes (SWNTs)

Table I: Summary of Reported Gravimetric Storage of H_2 in Various Carbon Materials.

Material	Reference	Max wt% H_2	T (K)	P (MPa)
SWNTs (low purity)	1	5–10	133	0.040
SWNTs (high-purity)	2	~4	300	0.040
GNFs (tubular)	4	11.26	298	11.35
GNFs (herringbone)	4	67.55	298	11.35
GNFs (platelet)	4	53.68	298	11.35
Graphite	4	4.52	298	11.35
GNFs	5	0.4	298–773	0.101
Li-GNFs	5	20.0	~473–673	0.101
Li-Graphite	5	14.0	~473–673	0.101
K-GNFs	5	14.0	<313	0.101
K-Graphite	5	5.0	<313	0.101
SWNTs (high purity)	3	8.25	80	7.18
SWNTs (~50% pure)	15	4.2	300	10.1

Note that the tubular graphite nanofibers (GNFs) apparently possess a tapering structure distinctly different from that of multi-walled nanotubes.
SWNTs = single-walled nanotubes.

https://doi.org/10.1557/S0883769400053458 Published online by Cambridge University Press

(Figure 1) in comparison with that of activated carbon, which has a high density of pores. Their work was initially stimulated by the theoretical description of capillarity in carbon nanotubes by Pederson and Broughton,[13] suggesting that gaseous species such as hydrogen might also be drawn into the capillaries of nanotubes. The carbon-nanotube samples used in the early work of Dillon et al.[1] were not characterized in detail and contained some amorphous carbon along with other carbon species and spent metal catalyst. The weight percent of SWNTs in their samples was not accurately known and was estimated to be in the 1–2-wt% range.[14] Through temperature-programmed desorption (TPD) measurements, the authors found that the hydrogen desorbed from both the nanotube and activated carbon samples at about the same temperature (~133 K). However, if they heated the nanotube sample in vacuum, a second peak appeared at a higher temperature (~290 K) in the TPD-versus-temperature spectrum, indicating that there was now a second type of adsorption/desorption site, which the authors suggested might be due to adsorption/desorption of H_2 trapped inside the SWNTs. This hydrogen can accumulate if the H_2 molecules have access to the nanotube cores through open tube tips. The open tubes presumably also allow a reversible process to occur through the desorption of H_2 that had previously been physisorbed in the central core of the carbon nanotubes. The authors did not see this high-temperature desorption site in either activated-carbon samples or in arc-generated soots produced without a catalyst. The SWNT constituent of the sample appeared to be especially effective for hydrogen adsorption. The activation energy for hydrogen desorption was found to be 19.62 J/mol, or approximately five times higher than that for a planar graphite surface, thereby promoting hydrogen-storage capacity at higher temperature. The hydrogen-storage capacity of this high-temperature site was estimated to be in the range of 5–10-wt% hydrogen (see Table I). This is equivalent to more than monolayer close-packed filling of H_2 inside the tubes, as discussed later. These authors[2,14] have recently developed a method to produce samples with a high concentration of short SWNTs with open ends that are accessible to the entry of hydrogen molecules. With these better characterized nanotube samples, they were able to achieve a more accurate determination of the hydrogen adsorption, which they estimated to be at ~4-wt% hydrogen at room temperature and 500-Torr hydrogen pressure. By opening and recapping the nanotubes, Dillon et al.[14] concluded that most of the hydrogen is stored within the capillary, rather than in the interstitial spaces between the SWNTs.

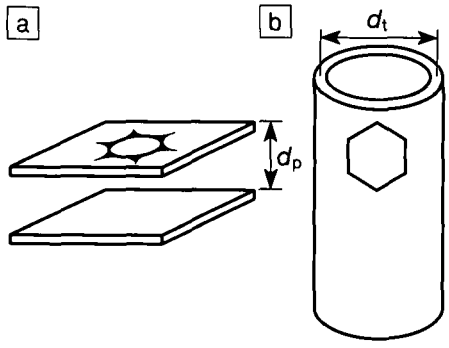

Figure 1. Two common pore geometries for hydrogen adsorption: (a) a slit pore with pore size d_p, and (b) a cylindrical pore (nanotube) with diameter d_t. Note that the carbon atoms inside the pore walls of actual nanotubes would have a honeycomb arrangement.

A similar hydrogen-storage capacity of 4.2 wt% was recently reported for SWNTs at a temperature of 300 K and pressure of 10.1 MPa.[15] In this study, SWNTs were synthesized by a semicontinuous hydrogen arc-discharge process, using a sulfur promoter. The sample (containing ~50% SWNTs) was treated by soaking in HCl and subsequent heat treatment at 500°C under vacuum. The relatively high hydrogen-storage capacity was attributed to the large mean tube diameter of about 1.85 nm. Calculations to verify the storage benefit of such large SWNT diameters are currently in progress and will be reported elsewhere.[16]

Ye et al. have undertaken experimental measurements of hydrogen adsorption on high-purity, "cut" SWNTs.[3] To cut the SWNT material and disrupt the tightly packed rope structure found in highly crystalline pristine SWNTs, a small quantity of material was sonicated in dimethylformamide and then extracted from the solvent by vacuum filtration. TEM revealed that this treatment broadens the diameter distribution of the SWNT ropes and also increases the number of SWNT terminations within ropes (hence the SWNTs are said to be "cut"); these differences were not evident in the x-ray-diffraction patterns of the material before and after the treatment, perhaps indicating that the average rope diameter was largely unchanged. The highest gravimetric hydrogen-storage capacity achieved in SWNT material treated in this manner was 8.25 wt%, at a temperature of 80 K and pressure of ~7 MPa (see Table I). At a pressure of ~4 MPa, a sudden increase in the adsorption capacities of the SWNT samples is reported; Ye and co-workers suspect that a structural phase transition is responsible for this effect. In their model, the ropes are split into individual tubes, thereby increasing the surface area available for physisorption.

More recently, Chen et al.[5] have reported high hydrogen adsorption in alkali-metal-doped GNFs at ambient pressure and slightly elevated temperatures. The GNFs used in this work were synthesized by catalytic decomposition of methane and reportedly exhibited a structure akin to a stack of cones (for this reason, we refer to them as nanofibers rather than nanotubes). Alkali-doped graphite was investigated, and it also exhibited remarkable hydrogen-storage capacity. Doping of the GNFs and graphite was carried out by means of solid-state reactions with Li- or K-containing compounds such as carbonates and nitrates; the final carbon-to-metal ratios in the GNF samples were reportedly 15:1, as determined by x-ray photoelectron spectroscopy (XPS). The extent of hydrogen uptake was determined by thermogravimetric analysis (TGA) and confirmed by TPD. Chen et al. reported dramatic enhancement of hydrogen storage in the alkali-doped systems, with best results found in the case of Li-GNFs and Li-graphite (20-wt% and 14-wt% gravimetric storage, respectively; see Table I). The remarkable storage improvement in Li-GNFs relative to the virtually negligible (0.4 wt%) storage in undoped GNFs was attributed by them to adsorption by means of a metal hydride interaction. Using *in situ* Fourier transform infrared (FTIR) spectroscopy, Chen and coworkers correlated an increase in intensity of the characteristic lithium hydride vibration at ~1420 cm^{-1} with increased hydrogen adsorption in the temperature range of 473–673 K. A new infrared band, which the authors attribute to C–H stretching vibrations, appeared in the spectral region of ~2600–3400 cm^{-1}; this feature was observed to disappear upon thorough desorption of hydrogen. Chen et al. suggested that an explanation for the remarkable boost in storage capacity may require dissociation of H_2, catalyzed by the intercalated alkali metal in the GNFs. Regarding the effect of repeated adsorption/desorption cycles, Chen et al. reported that the reduction in storage

capacity after 20 chemisorption and desorption cycles is only ~10%.

An independent measurement by Nützenadel et al.[17] of the *electrochemical* hydrogen-storage capacity of SWNTs was carried out using samples obtained from the MER Corporation (United States), CarboLex Inc. (United States), Dynamic Enterprise Ltd. (United Kingdom), tubes@rice (United States), and the research group of Patrick Bernier at the Université de Montpellier (France).[17] In each case, 20 mg of SWNTs were finely ground, mixed with 80 mg of Au powder (which serves as a compacting additive and does not participate in the electrochemical reaction), and pressed at a pressure of 500 MPa to form a pellet. In the experimental apparatus of Nützenadel et al., the SWNT/Au pellet served as the negative electrode, and a Ni plate was used to form the counter electrode. Experiments were conducted in a half-cell, using a solution of 6 M KOH as the electrolyte; potentials were referred to a $Hg/HgO/OH^-$ reference electrode. The hydrogen weight density was deduced from the amount of discharged current. Best results were obtained using as-prepared material from the Bernier group and chemically purified material from Dynamic Enterprise Ltd.; for these samples, the measured discharge capacities indicated storage of ~1.95-wt% hydrogen, but this value decreased by approximately 30% over 100 charge/discharge cycles. The effect of chemical post-treatment and/or metallic impurities on the absorptive capacity of the SWNT samples was not quantified in this work.

Simplistic Physical Arguments

To gain insight into the hydrogen-adsorption problem, it is first necessary to review a few basic facts about hydrogen molecules and the carbon surfaces to which they might bind. In the ground state, the hydrogen molecule is nearly spherical, with a kinetic diameter of 2.89 Å, and the intermolecular interactions between H_2 molecules are weak.[11,18] Therefore, H_2 molecules at elevated pressures on a solid surface are expected to assume a close-packed configuration. We use the parameters of the experimentally observed structure to provide one simple estimate for the maximum packing density for hydrogen molecules on a surface. Each molecule in this close-packed structure has six nearest neighbors, four in-plane and two out-of-plane. Experimentally, solid hydrogen at 4.2 K forms a hexagonal close-packed structure, with lattice parameters a = 3.76 Å and c = 6.14 Å,[19] so that c/a = 1.633, which is identical to $c/a = \sqrt{8/3}$ = 1.633 for the ideal hexagonal close-packing of spheres. This indicates that in the ground rotational state, the H_2 molecule is approximately spherical in shape.

Using purely geometric arguments, we can thus gain a simple geometric estimate for the close-packing capacity of hydrogen molecules above a plane of graphite. Graphite has a honeycomb structure, with an in-plane lattice parameter a_g = 2.46 Å and an interplanar separation of 3.35 Å. Since the value of the kinetic diameter for the hydrogen molecule is greater than a_g, the closest packing of hydrogen molecules on a graphite surface would have to be incommensurate with the graphene plane. Commensurate H_2 adsorption on a two-dimensional $\sqrt{3} \times \sqrt{3}$ graphene-based superlattice[20] (see Figure 2) would yield a lattice constant of a = 4.26 Å, which is significantly larger than that for the low-temperature close-packed structure of solid hydrogen.[19] The ratio of the number of hydrogen to carbon atoms (H:C) for the $\sqrt{3} \times \sqrt{3}$ commensurate stacking on a graphene surface would be H:C = 1:3. Given the 12:1 ratio between the masses of carbon to hydrogen, this commensurate stacking would yield ~2.8-wt% hydrogen for one layer of H_2 adsorbed on a single graphene layer. (This model might apply to describing monolayer deposition in a slit pore.)

In a real system, there are intermolecular forces and molecule-surface interactions that come into play, and there are also many edge states that might provide additional adsorption sites for the H_2 molecules. Neutron-scattering measurements[21] show that at sparse coverage, the commensurate $\sqrt{3} \times \sqrt{3}$ structure occurs (see Figure 2, top). A denser triangular structure, which is incommensurate with the graphite, is observed for higher hydrogen pressures (see Figure 2, bottom). Once a second layer begins to form, a lattice parameter of 3.51 Å is observed,[22] smaller than the value of 3.76 Å measured for the bulk hexagonal close-packing of hydrogen molecules in solid hydrogen. For this more dense two-layer phase, we obtain an estimate of H:C = 0.49, thus yielding a 4.1-wt% hydrogen adsorption on a flat sp^2 carbon surface.

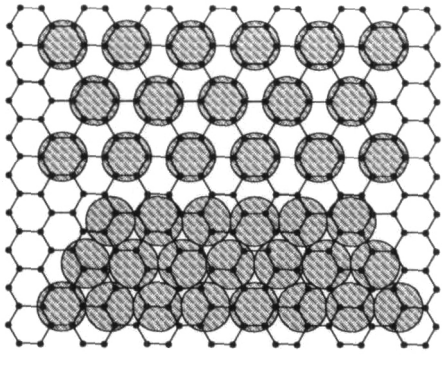

Figure 2. Relative density of a $\sqrt{3} \times \sqrt{3}$ commensurate (top) and an incommensurate (bottom) monolayer of H_2 on a graphite surface.[23]

Graphite intercalation compounds (GICs) have also been considered as a method for the uptake of hydrogen.[20] Although alkali-metal GICs (e.g., K, Rb, and Cs) are capable of the intercalation of H_2, the weight percent of hydrogen in the final compound for either a chemisorption[20,24–26] ($C_8KH_{2/3}$) or a physisorption[20,27] ($C_{24}KH_2$) process is too low to be of interest in the context of the DOE Hydrogen Plan. Recent experimental efforts using electrochemical techniques to intercalate hydrogen directly between the graphene layers[28] have been unsuccessful. These results are consistent with a molecular orbital calculation carried out by the same group showing that hydrogen ions, unlike lithium ions, do not form stable intercalation compounds because of the absence of three-dimensional p orbitals, which are presumably needed to bond the hydrogen to the adjacent graphene layer. However, the use of low concentrations of alkali metals (in a metal-to-carbon ratio of ~1:15) has been reported to catalyze high hydrogen uptake,[5] as already discussed.

Hydrogen Storage in Carbon Nanotubes

Two issues currently being debated are whether hydrogen adsorption in SWNTs is greater or less than that in slit pores, and whether hydrogen adsorption occurs in the interstitial channels between adjacent nanotubes in a rope of SWNTs. Neither of these issues has been conclusively settled at the present time.

Simple geometric arguments can be used to estimate the filling of a rope (crystalline lattice) of SWNTs. We present here two simple geometrical arguments. The first assumes the hydrogen to be a completely deformable fluid that fills the space not occupied by the carbon nanotube. Assume that we have a rope of (10,10)* nanotubes, each tube having a

*For an explanation of this nanotube symmetry notation, see Reference 31, Chapter 19.

https://doi.org/10.1557/S0883769400053458 Published online by Cambridge University Press

diameter of 13.8 Å and a unit cell dimension of 17.2 Å for the rope. This geometry yields an area of 147.4 $Å^2$ occupied by the nanotube and an area of 108.8 $Å^2$ of unoccupied area available for the hydrogen fluid. Assuming a hydrogen density of 0.071 g/cm^3 (corresponding to that of liquid hydrogen) and a density of 2.26 g/cm^3 for the carbon atoms within the nanotube volume yields a 2.3-wt% hydrogen uptake.

A second geometrical model takes into account the accessible volume to hydrogen molecules by considering the packing of hydrogen molecules of kinetic diameter 2.9 Å on the inner walls and in the interstitial volume of the nanotubes, as shown in Figure 3. For a (10,10) nanotube array, eight hydrogen molecules fit along the inside wall of the nanotube, which is estimated to have a diameter of (13.8 − 3.4) Å = 10.4 Å, taking into account the charge cloud of the π electrons at the inner carbon surface. The diameter of a circle through the center of the adsorbed hydrogen molecules is (10.4 − 2.9) Å = 7.5 Å. One hydrogen molecule fits into the interstitial volume of tubes with diameters greater than or equal to that of the (9,9) armchair tube. Using this geometrical model with close-packing of the H_2 molecules within the core of the (10,10) tube leads to 3.3-wt% hydrogen adsorption within the tube and 0.7-wt% adsorption within the interstitial space, or a total of 4.0-wt% hydrogen adsorption. As the tube diameter increases, the C–H van der Waals interaction at the wall interface decreases, but at the same time there is also an increase in the unoccupied central core volume, which for the (10,10) nanotube is described by the volume within a cylinder of diameter d_c (7.5 − 2.9) Å = 4.6 Å.

Some have argued that the curved inner surface of the tube leads to a reduction in the accessible geometric volume for the hydrogen, and detailed calculations in support of this viewpoint have been presented.[11] On the other hand, one can argue that under high-pressure conditions, the high compressibility of hydrogen and the attractive intermolecular interactions should lead to closer packing of hydrogen molecules, especially at low temperature. Detailed calculations in support of this concept have also been carried out,[8] yielding hydrogen densities higher than the simple geometric picture. This latter concept seems to be supported by the experimental observations of Dillon et al.[1,14]

We can further argue, using a 2.9-Å kinetic diameter for H_2, that hydrogen molecules should be adsorbed effectively within the interstitial space between nanotubes (see Figure 3). Since a hydrogen molecule in this interstitial space is in close proximity to three graphene surfaces, it therefore experiences a stronger surface attraction than on a single planar graphene surface, and this site would be expected to exhibit a higher binding energy.[23]

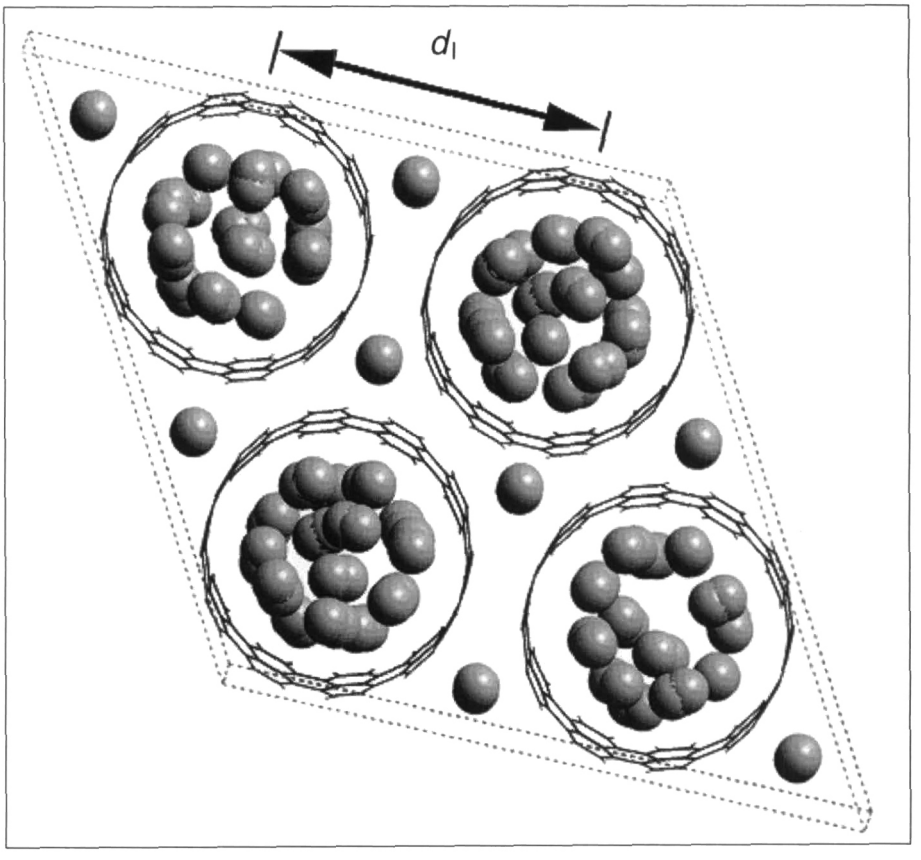

Figure 3. A typical configuration of H_2 molecules adsorbed on a triangular array of carbon nanotubes with a lattice constant of d_l. This configuration resulted from a classical Monte Carlo calculation in which the simulated storage pressure was 10 MPa and the simulated temperature was 50 K. The computed gravimetric storage capacity in this "periodic infinite lattice" is ~3.1-wt% H_2. The storage capacity in single-walled carbon nanotube geometries that are more compatible with the disordered, finite-diameter ropes observed by electron microscopy is currently being evaluated.[16]

Molecular-sieving calculations on the use of ropes of SWNTs for the separation of tritium from hydrogen indicate that the interstitial spaces between the nanotubes do provide suitable pores for hydrogen isotope separation;[29,30] the interstitial spaces, therefore, should also be available for direct hydrogen molecular adsorption. These calculations show that it should be possible to separate hydrogen (mass number 1) isotopes from tritium (mass number 3) when the nanopores are large enough to admit tritium but are too small to admit hydrogen.[29,30] Very similar theoretical results are obtained from a simple model for the adsorption of hard spheres and from more extensive path integral calculations.[29] These calculations indicate that nanotubes of ~6 Å diameter should show this quantum molecular-sieving phenomena for hydrogen and tritium isotopes. But since the smallest diameter for an actual nanotube appears to be ~7 Å (the diameter of C_{60}),[31,32] it is unlikely that SWNTs of sufficiently small diameters can be produced in adequate quantities to make quantum molecular sieves practical for hydrogen/tritium isotope separation. However, the calculations[29] further show that the interstitial channels or pores between the ordered SWNTs in a rope [such as a rope containing (10,10) nanotubes on a triangular lattice], can act as a quantum molecular sieve to

https://doi.org/10.1557/S0883769400053458 Published online by Cambridge University Press

separate hydrogen from tritium with high selectivity.[29] Experimental corroboration of this isotope-separation phenomenon would be of significant practical interest, especially because present isotope-separation methods are complicated and expensive.

Calculations of hydrogen uptake using a grand canonical ensemble Monte Carlo program show that hydrogen molecules can be adsorbed by van der Waals interactions inside a slit pore[11,20] or inside a carbon nanotube.[11] The calculations[11] show maximum hydrogen density within the pores for a pore size of ~7 Å in diameter for both the slit-pore and carbon-nanotube geometries. At this pore diameter, the hydrogen molecule fits between the slit-pore layers, and the molecule bonds to both sides of the slit pore, leading to strong capillary-adsorption forces. Simulations at 300 K predict a volumetric storage capacity of 4.3 kg/m^3 and 12.5 kg/m^3 for slit pores and nanotubes, respectively, corresponding to a total gravimetric hydrogen-storage capacity of 1.3 wt% for the slit pores and 1.1 wt% for the nanotubes. Simulations also predict that at low temperatures (150–200 K) and at a pressure of 10 MPa, the amount of hydrogen gas inside the slit pores could reach a density exceeding that of liquid hydrogen by 20%, with a total gravimetric storage capacity of ~4%. When these same calculational techniques are applied to SWNTs, a smaller adsorption capacity of ~1.3 wt% is obtained for the nanotubes. In general, these authors[11] reported that the nanotubes stored 30–60% less hydrogen than a slit pore for a gas pressure of 10 MPa and a pore diameter of 7 Å, but in special cases, the nanotube hydrogen uptake might be comparable with that for the slit pores. When hydrogen adsorption in the interstitial spaces between the tubes in a rope is also taken into account, carbon nanotubes may provide a better hydrogen-storage medium than slit pores. However, this issue is not yet settled, either experimentally or theoretically. Calculations using a variety of nanotube diameters and bundle geometries (including finite-sized bundles) will be reported elsewhere.[16]

Experimental results on activated carbons show a linear dependence of the excess hydrogen-adsorption capacity on the specific surface area of the activated carbons, in agreement with theory.[11] The maximum specific surface area measured for their activated carbon samples was 2290 m^2/g, yielding a maximum gravimetric storage capacity of 0.6 wt%, which compares well to the theoretical value of 0.7 wt% for the experimental adsorption conditions. At 77 K, a gravimetric storage capacity of 2-wt% and 5.5-wt% hydrogen was predicted for 10-Å-diameter nanotubes and slit pores, respectively.[11] On the basis of the Monte Carlo calculations and experimental measurements on characterized activated carbons under controlled conditions, these authors could not account for the large hydrogen uptake reported for slit pores[4] using physisorption models based on strong capillary forces within a nanopore.

Detailed model calculations have been carried out by Stan and Cole[7] for the adsorption of hydrogen in carbon nanotubes based on a Lennard-Jones potential model for the interaction between the hydrogen molecule and the nanotube.[7] For both graphite and carbon nanotubes, the adsorption potential of the hydrogen molecule is found to be more attractive at the center of the carbon hexagon than directly above a carbon atom, because more carbon atoms can participate in the binding. The calculations show that as the temperature falls below 77 K, the adsorption within the pore of the tube is very much more favorable than on a flat carbon surface (see Figure 2 of Reference 7), and it is believed that the quantum nature of the hydrogen molecule contributes to this low-temperature-enhanced adsorption within the nanotube. These authors also calculated a heat of absorption per particle of 1082 K for a (9,0) carbon nanotube, which has a tube diameter much smaller than that of experimentally available nanotubes. The calculated heat of adsorption per particle is significantly lower than the experimental determination of the heat of adsorption per particle of 2360 K measured by Dillon et al.[1] The reason for this discrepancy is not yet understood.

Calculations for H_2 adsorption at low coverage show that the interior curved surface of the nanotube actually absorbs substantially more H_2 than a flat graphitic sheet.[8] This calculation was carried out for a strongly curved (13,0) tube (d_t = 10.1 Å) somewhat smaller in diameter than the mean diameter of SWNTs currently being studied in the laboratory. When Stan and Cole[8] included a quantum correction to the effective wall H_2 potential, they found a further enhancement of the H_2 adsorption for $T < 75$ K.[8] Quantum mechanical behavior appears to be responsible for the enhanced H_2 absorption in SWNTs; no other form of carbon appears to exhibit this highly desirable property.

Other grand canonical ensemble Monte Carlo simulations based on a Lennard-Jones model potential[33] also found that the potential inside and outside of a SWNT was favorable for the adsorption of hydrogen. In these calculations, the nanotube diameter and nanotube separation were both varied to maximize the hydrogen adsorption. At an intertube separation of 0.334 nm, the greatest adsorption was found for a nanotube diameter of 1.96 nm. For a tube diameter of 1.17 nm, the hydrogen adsorption was found to increase when the intertube separation was increased from 0.344 nm to 0.7 nm. These types of calculations have the potential for refinement, as the experimental results become more quantitative and the model parameters and assumptions become more realistic.[7–10,29,33]

Although preliminary, the experimental results on the adsorption of hydrogen in open-ended single-walled carbon nanotubes are encouraging with regard to meeting the DOE Hydrogen Plan. On the other hand, the values given earlier[1,14] for the hydrogen capacity in single-walled carbon nanotubes are close to the limit of what seems feasible with our present state of knowledge. Still, the presently available single-walled nanotubes yield hydrogen-adsorption values near 4-wt% hydrogen uptake, which still needs to be increased by about 50% to meet the DOE plan, and this represents a significant technological future challenge.

Acknowledgments

The authors gratefully acknowledge the helpful discussions with Drs. G. Dresselhaus and A.M. Rao, Professors M. Endo and R. Saito, and Ms. M.R. Black. They are also thankful to many other colleagues for their assistance with the preparation of this article. The research at the Massachusetts Institute of Technology is supported by the National Science Foundation grant DMR 98-04734, and the work at the University of Kentucky is supported by NSF grants OSR-9452895 and DMR 98-09686 and by the University of Kentucky Center for Applied Energy Research. The authors also gratefully acknowledge support from DOE contract DE-AP05-98OR4287.

References

1. A.C. Dillon, K.M. Jones, T.A. Bekkedahl, C.H. Kiang, D.S. Bethune, and M.J. Heben, *Nature (London)* **386** (1997) p. 377.
2. A.C. Dillon, T. Gennett, J.L. Alleman, K.M. Jones, and M.J. Heben (private communication).
3. Y. Ye, C.C. Ahn, C. Witham, B. Fultz, J. Liu, A.G. Rinzler, D. Colbert, K.A. Smith, and R.E. Smalley, *Appl. Phys. Lett.* **74** (1999) p. 2307.
4. A. Chambers, C. Park, R.T.K. Baker, and N.M. Rodriguez, *J. Phys. Chem. B* **102** (1998) p. 4253.

5. P. Chen, X. Wu, J. Lin, and K.L. Tan, *Science* **285** (1999) p. 91.
6. S. Hynek, W. Fuller, and J. Bentley, *Int. J. Hydrogen Energy* **22** (1997) p. 601.
7. G. Stan and M.W. Cole, *J. Low Temp. Phys.* **110** (1998) p. 539.
8. G. Stan and M.W. Cole, *Surf. Sci.* **395** (1998) p. 280.
9. Q. Wang and J.K. Johnson, *J. Phys. Chem. B* **103** (1999) p. 277.
10. Q. Wang and J.K. Johnson, *J. Chem. Phys.* **110** (1999) p. 577.
11. M. Rzepka, P. Lamp, and M.A. de la Casa-Lillo, *J. Phys. Chem. B* **102** (1998) p. 10894.
12. J. Ouellette, in *Industrial Physicist* **5** (1) (American Institute of Physics, Woodbury, NY) p. 15.
13. M.R. Pederson and J.Q. Broughton, *Phys. Rev. Lett.* **69** (1992) p. 2689.
14. M.J. Heben (private communication).
15. C. Liu, Y.Y. Fan, M. Liu, H.T. Cong, H.M. Cheng, and M.S. Dresselhaus (unpublished).
16. K.A. Williams and P.C. Eklund (unpublished).
17. C. Nützenadel, A. Züttel, D. Chartouni, and L. Schlapbach, *Electrochem. Solid-State Lett.* **2** (1999) p. 30.
18. J.K. Kranendonk, *Solid Hydrogen* (Plenum Press, New York, 1983) p. 131.
19. In *Landolt-Börnstein Numerical Data and Functional Relationships in Science and Technology*, New Series III/14a, edited by K.-H. Hellwege and A.M. Hellwege (Springer-Verlag, Berlin, 1988) p. 18.
20. M.S. Dresselhaus and G. Dresselhaus, *Adv. Phys.* **30** (1981) p. 139.
21. N. Nielsen, J.P. McTague, and L. Passell, in *Phase Transitions in Surface Films*, edited by J.G. Dash and J. Ruvalds (Plenum Press, New York, 1979).
22. M. Nielsen, J.P. McTague, and W. Ellenson, *J. Phys.* **38** (1977) p. C4/10.
23. S.D.M. Brown, G. Dresselhaus, and M.S. Dresselhaus, in *Recent Advances in Catalytic Materials*, edited by N.M. Rodriguez, S.L. Soled, and J. Hrbek (Mater. Res. Soc. Symp. Proc. **497**, Warrendale, PA, 1998) p. 157.
24. M. Colin and A. Hérold, *Bull. Soc. Chim. Fr.* (1972) p. 1982.
25. G. Furdin, P. Lagrange, A. Hérold, and C. Zeller, *C.R. Acad. Sci. (Paris)* **282** (1976) p. C563.
26. T. Enoki, M. Sano, and H. Inokuchi, *J. Chem. Phys.* **78** (1983) p. 2017.
27. H. Inokuchi, N. Wakayama, T. Kondow, and Y. Mori, *J. Chem. Phys.* **46** (1967) p. 837.
28. M. Watanabe, M. Tachikawa, and T. Osaka, *Electrochim. Acta* **42** (1997) p. 2707.
29. Q. Wang, S.R. Challa, D.S. Sholl, and J.K. Johnson, *Phys. Rev. Lett.* **82** (1999) p. 956.
30. J.J.M. Beenakker, V.D. Borman, and S.Yu. Krylov, *Chem. Phys. Lett.* **232** (1995) p. 379.
31. M.S. Dresselhaus, G. Dresselhaus, and P.C. Eklund, *Science of Fullerenes and Carbon Nanotubes* (Academic Press, New York, 1996) p. 899.
32. S. Iijima and T. Ichihashi, *Nature (London)* **363** (1993) p. 603.
33. F. Darkrim and D. Levesque, *J. Chem. Phys.* **109** (1998) p. 4981. □

https://doi.org/10.1557/S0883769400053458 Published online by Cambridge University Press